J Therm Anal Calorim
DOI 10.1007/s10973-015-4890-8

Effect of *Ouratea* sp. butter in the crystallinity of solid lipids used in nanostructured lipid carriers (NLCs)

Juliana G. Galvão[1] · Gabriela G. G. Trindade[1] · Adriana J. Santos[1] · Raquel L. Santos[1] · Adriano B. Chaves Filho[2] · Ana Amélia M. Lira[1] · Sayuri Miyamoto[2] · Rogéria S. Nunes[1]

Received: 12 December 2014 / Accepted: 21 June 2015

Abstract The aim of this work was to evaluate the effect of *Ouratea* sp. butter (OB) on crystallinity of solid lipids used in nanostructured lipid carriers systems. Firstly, the composition of fatty acids in OB was evaluated by trans-esterification reaction for gas chromatography fatty acid methyl ester analysis. The solid lipids such as stearic acid (SA), beeswax (BW) and carnauba wax (CW) were submitted to recrystallization process (heating–cooling). Moreover, binary mixtures between solid lipids and OB were prepared in ratio 1:1 (w/w) by heating of the components above the melting point followed by cooling at room temperature. Thus, the samples were characterized by differential scanning calorimetry (DSC), thermogravimetry (TG), X ray diffraction (XRD) and hot-stage polarized optical microscopy (HSPOM). DSC curves showed a shift of the melting point to lower temperatures in the lipid mixtures with OB. TG data suggested a thermal stability reduction in the lipid mixtures containing SA and CW and an increase thermal stability in the mixture containing BW. XRD data confirmed DSC results, showing a reduction in intensity of main diffraction peaks of the lipid mixtures and a presence of the amorphous portion in angle 2θ: 22°. Finally, HSPOM demonstrated that the microstructures of solid lipids decreased in size and thickness in the mixtures containing OB at room temperature and slightly before the melting point, confirming previous characterizations. These results suggest that lipid mixtures with OB present a lower crystallinity, and it is expected that amorphous portion facilitates drug incorporation, for example.

Keywords *Ouratea* sp. butter · Solid lipids · Crystallinity · Nanostructured lipid carriers (NLCs) · Thermal analysis

Introduction

Over the years, pharmaceutical and cosmetic industries have made efforts to introduce new natural raw materials in the product development [1]. Recently, it was observed in northeast Brazil (Rio Grande do Norte—Latitude −05° 47′ 42″ and Longitude −35° 12′ 34″) the usage of seeds from *Ouratea* sp. tree by local people. After a rudimentary extraction procedure, butter can be obtained, which is generally used in food preparations. It is worth to mention that *Ouratea* sp. butter might be composed of saturated and unsaturated fats such as, essential fatty acids (e.g., oleic, palmitic and linoleic acids). These fatty acids can act as a potential emollient improving barrier function of the stratum corneum and consequently preventing transepidermal water loss (TEWL) favoring cutaneous hydration [2, 3]. In addition, vegetable oils and fats such as *Ouratea* sp. butter have recently been investigated in nanostructured formulations [4].

Therefore, *Ouratea* sp. butter (OB) becomes a potential lipid component in the nanostructured lipid carriers (NLC) development. NLCs, the second generation of lipid nanoparticles, consists in nanometric particles obtained from lipid mixtures between solid and semisolid or liquid lipids dispersed in a surfactant solution, maintaining solids at body and room temperature [5, 6].

✉ Juliana G. Galvão
julianaggalvao@gmail.com

[1] Pharmacy Department, Federal University of Sergipe, Av. Marechal Rondon, s/n, Cidade Universitária, São Cristóvão, SE 49000-100, Brazil

[2] Institute of Chemistry, University of São Paulo, São Paulo, SP 05508-000, Brazil

Published online: 08 July 2015

The main advantages of these systems include protection of labile substances from chemical degradation, control of release of substances due to the solid state of the lipid matrix, low toxicity and formation of films over the skin showing occlusive properties [7–9].

The selection of the lipid mixture is crucial step for the NLC production with physicochemical characteristics suitable for its application. It has been reported that lipid mixture presents a great impact in the chemical stability of bioactive substances [10, 11]. Moreover, the addition of oil or fats to a solid lipid creates a less ordered crystal lattice with an increased number of imperfections, which can accommodate drug clusters, for example. In selecting lipids for NLC development, it is necessary to consider the compatibility between solid and liquid lipids. Kasongo and co-workers [12] used the differential scanning calorimetry (DSC) in order to determine the interaction between solid and liquid lipids in a binary mixture. The stability related to chemical degradation (e.g., oxidation and lipolysis) of the lipid phase should be considered as well. Furthermore, the lipids should be biodegradable, be non-toxic and be capable of producing particles in nanometric range [8, 12, 13].

Thus, the aim of this work is to evaluate the effect of the *Ouratea* sp. butter in the crystallinity of solid lipids used in nanostructured lipid carriers systems by differential scanning calorimetry (DSC), thermogravimetry (TG), X ray diffraction (XRD) and hot-stage polarized optical microscopy (HSPOM).

Materials and methods

Materials

Stearic acid, beeswax and carnauba wax were purchased at Dinâmica. *Ouratea* sp. butter was kindly provided by Raros Naturals® (Macaíba/RN Brazil).

Ouratea sp. butter composition by FAME analysis

The composition of fatty acids in *Ouratea sp*. butter was evaluated by transesterification reaction for gas chromatography fatty acid methyl ester (FAME) analysis as previously described by Masood et al. [14]. Butter samples (10.0 ± 0.1 mg; $n = 3$) were mixed with methanol (1.75 mL), heneicosanoic acid 1 mg mL^{-1} (C21:0; 100 µL) and acetyl chloride (100 µL), and heated for 60 min at 100 °C. After cooling, hexane (1.5 mL) was added and the tubes were vortexed for 1 min and centrifuged at $1500 \times g$ for 2 min at 4 °C. The upper organic phase was collected, and the samples were extracted again with hexane (0.7 mL). The upper organic phase was collected, combined and evaporated under nitrogen to dryness, and the dry residue was then dissolved in 500 µL of hexane. Individual FAMEs were analyzed by injecting 1 µL of the sample into a GC with flame ionization detection on a Trace 1310 (Thermo Scientific) using a capillary column (DB-FFAP, 15 m × 0.1 mm ID × 0.1 µm film thickness, Agilent Technologies). The temperature program started with an initial temperature of 150 °C with a 0.25-min hold, which was increased with 35 °C min^{-1} to 200 °C, 8 °C min^{-1} to 225 °C with a 3.2-min hold, and then 80 °C min^{-1} to 245 °C followed by an 4.75-min isothermal period. Additional instrumental conditions: hydrogen/nitrogen was used as carrier gas at constant pressure of 345 kPa. FID set at 250 °C, air and nitrogen makeup gas flow 350 and 40 mL min^{-1}; split ratio at 30:1; autosampler injections of 1-µL volume. Run time for a single sample was 13 min. FAME was identified by direct comparison with a FAME standard mix (Supelco 37 Component FAME Mix; Sigma-Aldrich), and each individual peak was integrated and normalized by the internal standard. The percentage of individual FAME was calculated in relation to the total area of FAME peaks.

Sample preparation

The solid lipids, stearic acid (SA), beeswax (BW) and carnauba wax (CW) were heated, above their melting points of 58, 63 and 82 °C, respectively. Thereafter, they were cooled to room temperature (recrystallization process). To prepare the binary mixtures, the solid lipids (SA, BW, CW) and the OB were heated and melted at the temperature of 85 °C, then mechanically mixed for 5 min, subsequently cooled down, and mixed until solidification. The binary mixtures were prepared in the 1:1 ratio, since this is the optimal concentration, resulting in a mixture of crystals with a high degree of disorder [15]. After these procedures, the samples were sent to characterizations.

Characterizations: differential scanning calorimetry (DSC)

DSC curves were obtained using DSC 2010 TA Instruments equipment. The analysis were performed in the range of 25–200 °C, under heating rate of 10 °C min^{-1} and dynamic nitrogen atmosphere (50 mL min^{-1}) using approximately 3 mg of the sample in aluminum crucibles.

Thermogravimetry (TG)

TG analysis was performed by using TA Instruments TG/DTA 2960 SDT equipment. TG curves were acquired in the range 25–800 °C, under heating rate of 10 °C min^{-1} and under dynamic nitrogen atmosphere (50 mL min^{-1})

using approximately 10 mg of the sample in platinum crucibles.

X ray diffraction (XRD)

X ray diffraction analysis were performed in Rigaku diffractometer using Co K_α ($\lambda = 1.79$ Å), 40-kV voltage and 30 mA. The measurements were obtained in the range 10°–80° and scanning rate of 1° min^{-1}.

Hot-stage polarized optical microscopy (HSPOM)

The samples such as, SA, BW, CW and their binary mixtures with OB were examined under a polarizing light with an Ortoplan–Pol model by Ernst Leitz GmbH microscope, coupled to a digital camera Kodak (DC4800 model) and equipped with an in situ hot stage (two-stage system for temperature control HS1 model by Instec Co.). The samples were deposited between two glass plates to obtain specimens with similar thicknesses (under 10 μm). In order to compare them with the DSC experiments, the samples were heated above their melting point and then cooled to room temperature and then re-heated above melting point. Observations from the first cooling and second heating were recorded [16]. All samples were observed using 20× magnification.

Results and discussion

On the basis of results obtained in the analysis of the *Ouratea* sp. butter composition, nine fatty acids were identified (Table 1). The predominant fatty acids were C16:0 palmitic (34.7 %), C18:1n-9 oleic (31.8 %), C14:0 miristic (14.4 %) and C18:2n-6 linoleic (11.6 %), and minor amounts of other fatty acids such as, C18:0 stearic (4.2 %), C12:0 lauric (1.9 %), C17:0 margaric (0.3 %), C18:3n-3 α-linolenic (0.1 %) and C20:1n-9 eicosenoic (0.2 %) were identified. These results are in agreement with Attama et al. [17] where long-chain fatty acids ranging from C14 to C24 are common to animal and vegetable oils and fats.

Table 1 Fatty acid composition of raw *Ouratea* sp. butter obtained from FAME analysis

Fatty acids (% of total fatty acids) in raw *Ouratea* sp. butter	
C12:0—lauric	1.9 ± 0.01
C14:0—miristic	14.4 ± 0.3
C16:0—palmitic	34.7 ± 0.6
C17:0—margaric	0.3 ± 0.01
C18:0—stearic	4.2 ± 0.1
C18:1n-9—oleic	31.8 ± 0.4
C18:2n-6—linoleic	11.6 ± 0.9
C18:3n-3—α-linolenic	0.1 ± 0.01
C20:1n-9—eicosenoic	0.2 ± 0.01

± Standard deviation

DSC is an important tool to characterize raw materials used in NLCs formulations, providing information related to physical state and crystallinity of the sample through thermal behavior. This technique also allow us to evaluate the main process parameters used in the NLCs preparation once the lipid mixture is heated and after cooled (recrystallized) for NLCs formation [18]. Based on NLCs preparation process, the solid lipid underwent recrystallization process (heating–cooling) in order to evaluate possible modifications during the NLCs production process.

DSC curves regarding solid lipids before and after recrystallization process are shown in the Fig. 1. SA presents only one endothermic peak in the range of 40–65 °C ($T_{peak} \sim 58$ °C), which is related to melting point [19, 20]. In the Fig. 1, it is also possible to observe that even after recrystallization process the SA does not present great changes in the melting point (58 °C). According to Desai et al. [21], these observations refer to the ability of SA to return to its original crystalline form, after recrystallization. Like SA, BW and CW do not present changes in the melting point ($T_{peak} \sim 63$ and 82 °C, respectively) as well [16, 22]. These results make SA, BW and CW potential solid lipids for NLCs formulations [23]. Given that due to the high melting point of CW compared with others, the

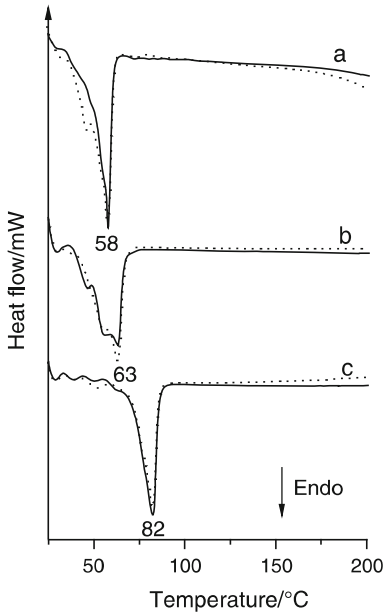

Fig. 1 DSC curve before (*solid line*) and after (*dash line*) recrystallization process of the stearic acid (*a*), beeswax (*b*), carnauba wax (*c*)

use of CW can be limited for some NLCs preparations methods like solvent diffusion method.

Figure 2 demonstrates that OB has four endothermic events: 1° in the range of 30–40 °C (T_{peak} ~ 35 °C), 2° in the range of 40–50 °C (T_{peak} ~ 48 °C), 3° in the range of 50–68 °C (T_{peak} ~ 60 °C) and 4° in the range of 70–80 °C (T_{peak} ~ 75 °C). From the OB composition analysis, it was possible to suggest that these endothermic events probably correspond to lauric, myristic, palmitic and stearic acids, which present melting points approximately at 44.9, 54.7, 63 and 71.2 °C, respectively [24–26].

DSC curve of the physical mixture between SA + OB (e) showed an overlapping of the two isolated compounds curves, which SA endothermic peak presented a slight shift to lower temperature (T_{peak} ~ 50 °C), and other endothermic peak (T_{peak} ~ 34 °C) related to OB showed a slight shift to lower temperature as well. Moreover, physical mixture between BW + OB and CW + OB also showed an overlapping of the compounds in which solid lipids (BW and CW) endothermic peaks (T_{peak} ~ 58 and 80 °C, respectively) and other endothermic peak related to OB endothermic event (30 and 34 °C). These shifts to lower melting temperatures in the physical mixtures suggest that OB promoted a crystalline disorder in the lipid matrix [17]. According to Villalobos-Hernandez and Müller-Goymann [22], these results are due to the presence of a semisolid or liquid lipid, which prevents entire crystal rearrangement of solid lipids.

TG curves related to solid lipids before and after recrystallization are shown in Fig. 3. This figure represents mass variation of solid lipid samples (SA, BW and CW) before and after recrystallization. SA has shown two losses in mass, the first in the range of 161–306 °C (Δm_1 = 79.63 % T_{peak} DTG ~ 267 °C) and the second in the range of 306–410 °C (Δm_2 = 16.56 % T_{peak} DTG ~ 380 °C) both characteristic of SA decomposition. In addition, BW presented only one loss in mass in the range of 180–480 °C (Δm_1 = 99.5 % T_{peak} DTG ~ 396.7 °C). CW also showed only one loss in mass in the range of 250–500 °C (Δm_1 = 98.5 % T_{peak} DTG ~ 426.1 °C). It is suggested that even after recrystallization process, great changes in thermal degradation were not present for solid lipids [27].

OB showed two main loss in mass, first in the range of 240–270 °C (Δm_1 = 1.21 % and T_{peak} DTG ~ 259 °C) and second in the range of 300–483 °C (Δm_2 = 97.06 % and T_{peak} DTG ~ 414 °C). In the TG curves of physical mixture between OB and SA, it was possible to observe three losses in mass: 1° in the temperature range of 156–306 °C (Δm_1 = 41.10 % and T_{peak} DTG ~ 258 °C), 2° in the range of 306–424 °C (Δm_2 = 52.62 % and T_{peak} DTG ~ 399 °C) and 3° in the range of 424–466 °C (Δm_3 = 4.52 % and T_{peak} DTG ~ 446 °C). In addition, physical mixtures of OB + BW and OB + CW presented only one mass loss event in the range of 180–480 °C (Δm_1 = 99.5 % T_{peak} DTG ~ 409 °C) and 250–500 °C (Δm_1 = 98.5 % T_{peak} DTG ~ 410 °C). Although TG data suggest a decrease in thermal stability in the lipid mixture containing SA and CW, an increase in thermal stability was observed in the OB + BW mixture when compared with pure solid lipids [27] (Fig. 4).

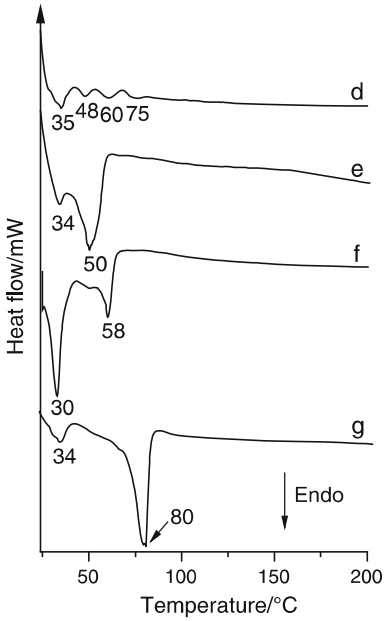

Fig. 2 DSC curve of the *Ouratea* sp. butter (*d*), physical mixtures: butter + stearic acid (*e*), butter + beeswax (*f*), butter + carnauba wax (*g*)

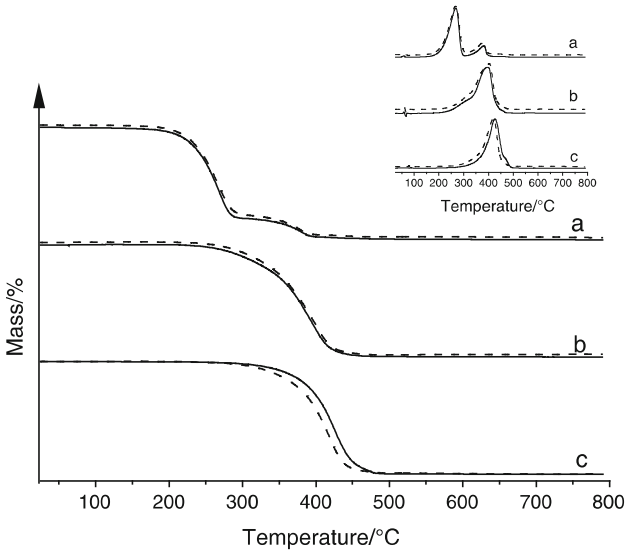

Fig. 3 TG curve before (*solid line*) and after (*dash line*) recrystallization process of the stearic acid (*a*), beeswax (*b*) and carnauba wax (*c*) (*Inset* derivative thermogravimetric curves of the samples)

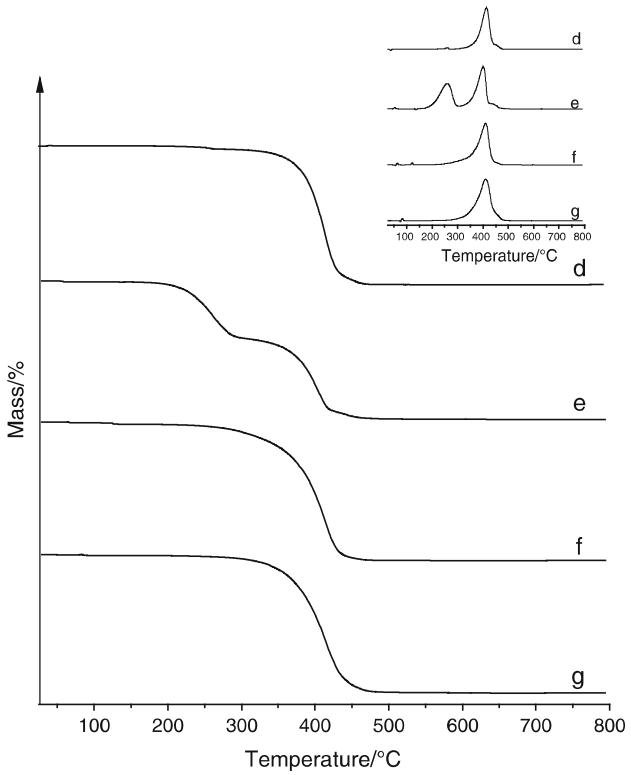

Fig. 4 TG curve of the O*uratea* sp. butter (*d*), physical mixtures: butter + stearic acid (*e*), butter + beeswax (*f*), butter + carnauba wax (*g*) (*inset* derivative thermogravimetric curves of the samples)

X ray diffraction corresponding to solid lipids before and after recrystallization is shown in the Fig. 5. Solid lipids presented main diffraction peaks at 2θ angle of SA (23.87°; 25.00°; 27.92°), BW (22.55°; 25.14°; 28.04°) and CW (25.28°; 27.92°). It is important to stress that even after recrystallization process, great changes in the main diffraction peaks of solid lipids were not observed, confirming data obtained from DSC analysis.

OB presented a broad peak and other small peak at 2θ angle of 20° and 23°, respectively. Moreover, lipid mixtures between OB and solid lipids demonstrated that there occurred an overlapping of diffraction profiles with predominance of peaks observed in pure solid lipids. Additionally, these lipid mixtures presented a small amorphous portion about at 2θ angle of 22° which does not appear in the pure lipid solids. According to Attama and Müller-Goymann [28], these results suggest that lipid matrix formed has lower crystallinity and it is expected that amorphous portion facilitates drug incorporation, for example. Furthermore, it has a decrease in the main diffraction peaks intensities of the lipid mixtures containing OB when compared with solid lipids, highly ordered.

XRD analysis confirmed data obtained from DSC in which lipid mixtures with OB demonstrated melting point shifts to lower temperatures in comparison with pure solid lipids (Fig. 6).

HSPOM is an analytical technique used in the characterization of lipids to observe the microstructural changes in fats during melting, as the lipid passes from crystalline phase to isotropic phase [17]. Figure 7 presents the samples OB (a), the solid lipids SA (b), BW (d), CW (f) and their physical mixtures with OB (c, e, g, respectively) at room temperature (RT), slightly before and after the melting

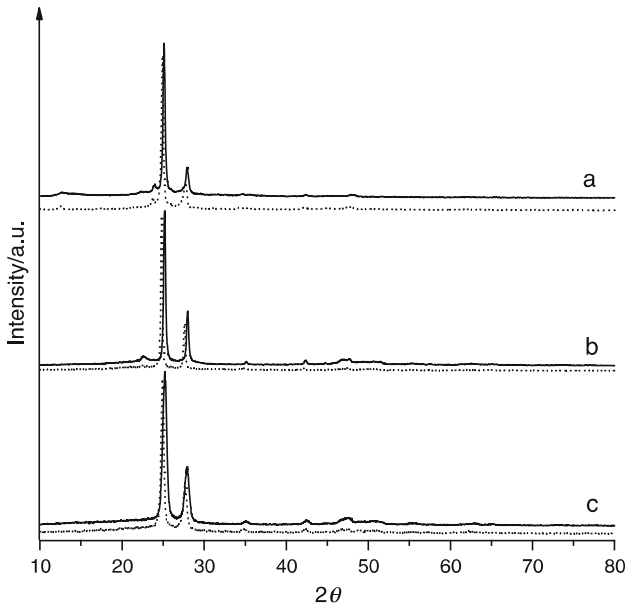

Fig. 5 X ray diffraction before (*solid line*) and after (*dash line*) recrystallization process of the stearic acid (*a*), beeswax (*b*) and carnauba wax (*c*)

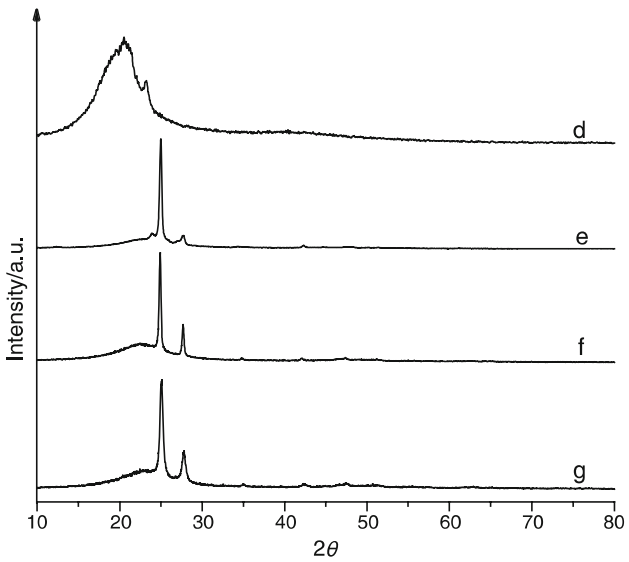

Fig. 6 X ray diffraction of the O*uratea* sp. butter (*d*), physical mixtures: butter + stearic acid (*e*), butter + beeswax (*f*), butter + carnauba wax (*g*)

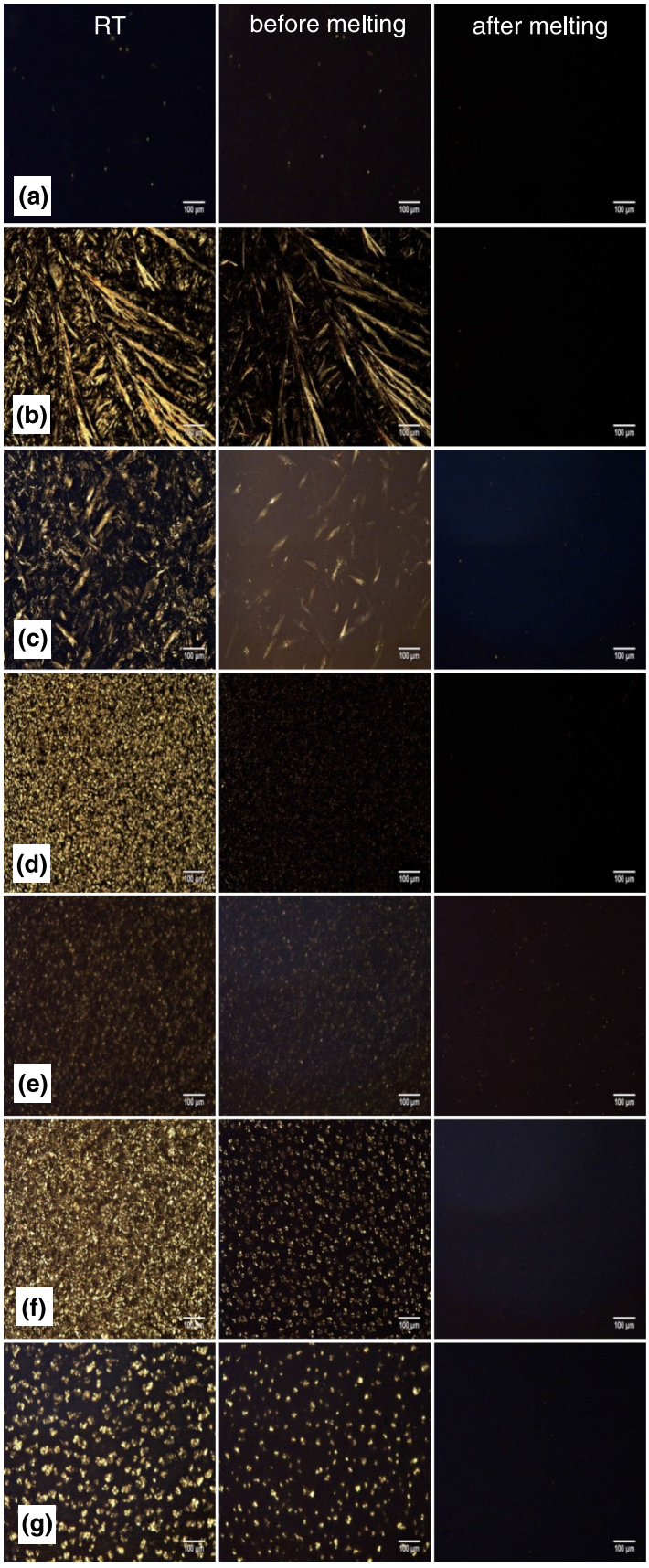

Fig. 7 Optical micrographs performed in HSPOM corresponding to complete crystallization process from 85 to 25 °C (room temperature—RT) of the *Ouratea* sp. butter (**a**); the pure solid lipids, stearic acid (**b**), beeswax (**d**), carnauba wax (**f**) and their binary mixtures in the ratio of 1:1 butter + stearic acid (**c**), butter + beeswax (**e**), butter + carnauba wax (**g**). *Bar* represents 100 μm

point. The OB presents an isotropic phase in all tested temperatures. At RT, the microstructure appears highly ordered in pure solid lipids, as well as, beforehand characterizations. SA and BW exhibited needle-shaped structure, and CW clearly presented maltese cross-characteristic of lamellar structure. In both RT and slightly before the melting point, these microstructures decreased in size and thickness in the mixtures containing OB, suggesting a lower crystallinity as it was observed at the previous characterizations. Likewise, after the melting point in all samples, these microstructures disappear with increasing temperature leaving the place to an amorphous state (isotropic phase) (Fig. 7).

Conclusions

Based on the results in this work, it is possible to conclude that even after recrystallization the solid lipids remained its crystal structure. In addition OB was capable of decreasing solid lipids (SA, BW and CW) crystallinity. From DSC analysis, it was observed that lipid mixtures with OB presented melting point shifts to lower temperatures when compared with pure solid lipids. TG data suggested a decrease in thermal stability of lipid mixtures containing SA and CW, but an increase in the thermal stability of mixture containing BW. XRD data showed a decrease in the main diffraction peaks in the lipid mixtures containing OB when compared with highly ordered solid lipids, as well as, the presence of an amorphous portion at 2θ of 22°. Furthermore, these results confirmed the data obtained from DSC in which lipid mixtures presented melting point shifts to lower temperatures when compared with pure solid lipids. Finally, HSPOM demonstrated that the microstructures of solid lipids decreased in size and thickness in the mixtures containing OB, suggesting a lower crystallinity as well. Thus, it is suggested that lipid matrix has a lower crystallinity and it is expected that amorphous portion facilitates drug incorporation, for example.

Acknowledgements The authors acknowledge the Conselho Nacional de Desenvolvimento Científico e Tecnológico (CNPq/Brazil), the Coordenação de Aperfeiçoamento de Pessoal de Nível Superior (CAPES/Brazil), and the Fundação de Apoio à Pesquisa do Estado do Rio Grande do Norte (FAPERN/Brazil PAPPE INTEGRAÇÃO—INOVA-RN No 001/2011) for supporting funds. We are grateful to Raros Naturals® (Macaíba/RN Brazil) for providing the *Ouratea* sp. butter used in this study. This work benefited from the hot-stage polarized optical microscopy facilities of the Complex Fluid Group (Institute of Physics, University of São Paulo/Brazil).

References

1. Duber-Smith DC, Chang YH, Olson AB, Rosholt AP, Api AM, Vey M, Ugurlayan AM, Srinivasan V, Antignac E, Troyano E, Mcmillan D, Sarlo K, Li L, Wimalasena R, Flanagan J, Garrison M., Dayan N, Kilfoyle BE, Tere JK. Natural Cosmetics. Kirk-Othmer Encycl Chem Technol. 2012. doi:10.1002/0471238961.natudaya.a01.
2. Fernandes RD. Estudo Químico e Atividades Biológicas de *Ouratea hexasperma var. planchonii Engl.* (Ochnaceae). Dissertação–Programa de Pós-Graduação em Química, Área de Concentração em Química de Produtos Naturais. Seropédica, Universidade Federal Rural do Rio de Janeiro; 2008.
3. Suzart LR, Daniel JFS, Carvalho MG. Biodiversidade flavonoídica e aspectos farmacológicos em espécies dos gêneros *Ouratea* e *Luxemburgia* (Ochnaceae). Quím Nova. 2007;30(4):984–7.
4. Badea G, Lacatuşu I, Badea N, Ott C, Meghea A. Use of various vegetable oils in designing photoprotective nanostructured formulations for UV protection and antioxidant activity. Ind Crops Prod. 2015;67:18–24.
5. Müller RH, Petersen RD, Hommoss A, Pardeike J. Nanostructured lipid carriers (NLC) in cosmetic dermal products. Adv Drug Deliv Rev. 2007;59(6):522–30.
6. Partidar A, Thakur DS, Kumar P, Verma JA. A review on novel lipid based nanocarriers. Int J Pharm Pharm Sci. 2010;2(4):30–5.
7. Guterres SS, Alves MP, Pohlmann AR. Polymeric nanoparticles, nanospheres and nanocapsules, for cutaneous applications. Drug Target Insights. 2007;2:147–57.
8. Müller RH, Mäder K, Gohla S. Solid lipid nanoparticles (SLN) for controlled drug delivery—a review of the state of the art. Eur J Pharm Biopharm. 2000;50(1):161–77.
9. Mehnert W, Mäder K. Solid lipid nanoparticles. Adv Drug Deliv Rev. 2012;64:83–101.
10. Müller RH, Radtke M, Wissing SA. Solid lipid nanoparticles (SLN) and nanostructured lipid carriers (NLC) in cosmetic and dermatological preparations. Adv Drug Deliv Rev. 2002;1:131–55.
11. Mitri K, Shegokar R, Gohla S, Anselmi C, Müller RH. Lipid nanocarriers for dermal delivery of lutein: preparation, characterization, stability and performance. Int J Pharm. 2011;414(1–2):267–75.
12. Kasongo KW, Pardeike J, Müller RH, Walker RB. Selection and characterization of suitable lipid excipients for use in the manufacture of Didanosine-loaded solid lipid nanoparticles and nanostructured lipid carriers. J Pharm Sci. 2011;100:5185–96.
13. Doktorovová S, Araújo J, Garcia ML, Rakovský E, Souto EB. Formulating fluticasone propionate in novel PEG-containing nanostructured lipid carriers (PEG-NLC). Colloids Surf B Biointerfaces. 2010;75(2):538–42.
14. Masood A, Stark KD, Salem N Jr. A simplified and efficient method for the analysis of fatty acid methyl esters suitable for large clinical studies. J Lipid Res. 2005;46:2299–305.
15. Zheng M, Falkeborg M, Zheng Y, Yang T, Xu X. Formulation and characterization of nanostructured lipid carriers containing a mixed lipids core. Colloids Surf A Physicochem Eng Asp. 2013;430:76–84.
16. Gaillard Y, Mija A, Burr A, Darque-Ceretti E, Felder E, Sbirrazzuoli N. Green material composites from renewable resources: polymorphic transitions and phase diagram of beeswax/rosin resin. Thermochim Acta. 2011;521(1–2):90–7.
17. Attama AA, Schicke BC, Müller-Goymann CC. Further characterization of theobroma oil-beeswax admixtures as lipid matrices for improved drug delivery systems. Eur J Pharm Biopharm. 2006;64(3):294–306.

18. Souza ALR. Desenvolvimento de nanopartículas lipídicas sólidas contendo Praziquantel. Tese (Doutorado em Ciências Farmacêuticas)—Faculdade de Farmácia, Araraquara, Universidade Estadual Paulista "Júlio Mesquita Filho"; 2011.
19. Chen Z, Cao L, Shan F, Fang G. Preparation and characteristics of microencapsulated stearic acid as composite thermal energy storage material in buildings. Energy Build. 2013;62:469–74.
20. Rowe RC, Sheskey PJ, Owen SC. Handbook of pharmaceutical excipients. London: The Royal Pharmaceutical Society of Great Britain and The American Pharmaceutical Association; 2009. p. 697–9.
21. Desai D, Kothari S, Huang M. Solid-state interaction of stearic acid with povidone and its effect on dissolution stability of capsules. Int J Pharm. 2008;354(1–2):77–81.
22. Villalobos-Hernández JR, Müller-Goymann CC. Novel nanoparticulate carrier system based on carnauba wax and decyl oleate for the dispersion of inorganic sunscreens in aqueous media. Eur J Pharm Biopharm. 2005;60(1):113–22.
23. Kheradmandnia S, Vasheghani-Farahani E, Nosrati M, Atyabi F. Preparation and characterization of ketoprofen-loaded solid lipid nanoparticles made from beeswax and carnauba wax. Nanomedicine. 2010;6(6):753–9.
24. Fauzi H, Metselaar HSC, Mahlia TMI, Silakhori M, Nur H. Phase change material: optimizing the thermal properties and thermal conductivity of myristic acid/palmitic acid eutectic mixture with acid-based surfactants. Appl Therm Eng. 2013;60:261–5.
25. Tarate B, Bansal AK. Characterization of CoQ 10-lauric acid eutectic system. Thermochim Acta. 2015;605:100–6.
26. Teixeira ACT, Garcia AR, Ilharco LM, Silva AMPSG, Fernandes AC. Phase behaviour of oleanolic acid, pure and mixed with stearic acid: Interactions and crystallinity. Chem Phys Lipids. 2010;163:655–66.
27. Almeida AE, Souza ALR, Cassimiro DL, Gremião MDPD, Ribeiro CA, Crespi MS. Thermal characterization of solid lipid nanoparticles containing praziquantel. J Therm Anal Calorim. 2012;108:333–9.
28. Attama AA, Müller-Goymann CC. Effect of beeswax modification on the lipid matrix and solid lipid nanoparticle crystallinity. Colloids Surf A Physicochem Eng Asp. 2008;315(1–3):189–95.